Journal of Non-Crystalline Solids 358 (2012) 571–576

Contents lists available at SciVerse ScienceDirect

Journal of Non-Crystalline Solids

journal homepage: www.elsevier.com/ locate/ jnoncrysol

Morphology of swift heavy ion tracks in metallic glasses

M.D. Rodríguez [a,*], B. Afra [a], C. Trautmann [b], M. Toulemonde [c], T. Bierschenk [a], J. Leslie [a], R. Giulian [a], N. Kirby [d], P. Kluth [a]

[a] Research School of Physics and Engineering, The Australian National University, Canberra ACT 0200, Australia
[b] Gesellschaft für Schwerionenforschung (GSI), 64291 Darmstadt, Germany
[c] Centre interdisciplinaire de recherche sur les Ions, les Materiaux et la Photonique (CIMAP), Caen, France
[d] Australian Synchrotron, Melbourne, VIC 3168, Australia

ARTICLE INFO

Article history:
Received 12 August 2011
Received in revised form 21 October 2011
Available online 17 November 2011

Keywords:
Metallic glasses;
Ion tracks;
Small angle X-ray scattering;
Amorphous metals;
Radiation damage

ABSTRACT

Swift heavy ion irradiated metallic glasses were studied using synchrotron based small angle X-ray scattering (SAXS). Ribbons of $Fe_{80}B_{20}$, $Fe_{85}B_{15}$, $Fe_{81}B_{13.5}Si_{3.5}C_2$ and $Fe_{40}Ni_{40}B_{20}$ were irradiated with 11.1 MeV/nucleon (MeV/u) ^{132}Xe, ^{152}Sm, ^{197}Au and 8.2 MeV/u ^{238}U ions to fluences between 1×10^{10} and 1×10^{12} ions/cm^2. The SAXS measurements provide evidence for the formation of ion tracks and allow a quantitative analysis of the track ensemble in all studied materials. The ion tracks have been well described by cylinders with abrupt boundaries and an electronic density change of (0.03 ± 0.01)% between track and matrix material. An inelastic thermal spike model was fitted to the experimental track radii to determine the critical energy density required to create an ion track. Despite the similar energy loss and track cross-sections, 30% higher track creation threshold is apparent for the binary alloys.

1. Introduction

Amorphous metals, also called metallic glasses, are metallic alloys with a disordered non-crystalline atomic structure. The amorphous structure is quenched from the liquid state by rapid cooling with rates of 10^5 to 10^6 K/s. While they are technically glasses, amorphous metals are much tougher and less brittle than oxide glasses and ceramics. There is a high level of interest in metallic glasses due to their interesting physical properties such as high mechanical strength, great wear and corrosion resistance, and high elasticity [1–3]. Taking advantage of such properties, there has been increasing utilization of amorphous metals in diverse applications in recent years such as magnetic cores for high frequency electronics, micro-electromechanical systems (MEMS), sporting equipment, medical and aerospace applications [4]. The metallic glasses studied in this work are used as cores of magnetic switches, employed in heavy ion induction linear accelerators [5]. The study of ion irradiation induced structural changes in amorphous metals provides insights into the radiation resistance of these materials which is essential for an efficient utilization in such applications.

High electronic excitations generated by swift heavy ion irradiation (SHII) of a solid can lead to the formation of long columnar defects along the ion trajectories, termed "ion tracks" [6–9]. Such ion tracks have been observed in numerous insulators [10–12], metals [13,14] and semiconductors [15–18]. Metallic materials are in general less sensitive to SHII due to their high electron mobility, with the exception of a few selected metals (e.g. Bi [19], Zr, Co, Ti [20] and Fe [21,22]), crystalline alloys [23] and various amorphous metallic alloys [24–33]. Evidence for the sensitivity of amorphous metals to SHII was demonstrated by Klaumünzer et al. [24,25,31], who observed the appearance of irreversible anisotropic plastic deformation. Klaumünzer *et al.* showed that, under SHII the dimensions of amorphous samples shrink parallel and expanded perpendicular to the direction of the ion beam without any apparent volume change. This phenomenon, also known as "ion hammering", becomes measurable at high fluences with significant track overlap [31] above a material dependent threshold value for the electronic energy loss (S_e). According to a "thermal spike" description [34–36], an ion track in an amorphous material represents a cylindrical mesoscopic defect in the form of a strained thermo-elastic inclusion and thus consists of a modified amorphous state. Another macroscopic SHII-induced effect in amorphous metallic alloys is the increase in electrical resistivity. *In situ* resistivity measurements on $Fe_{85}B_{15}$ revealed this damage effect at significantly lower fluences than the ion hammering effect [36], above an electronic energy loss threshold of $S_e = 14$ keV/nm. Damage cross-sections were deduced by analyzing the evolution of the electrical resistivity versus fluence [26], and track radii were calculated [28] assuming that the defects are created in a cylinder along the ion path. However the above methods measure integral changes and a direct access to the track structure of individual tracks still remains challenging.

* Corresponding author. Tel.: +62 2 6125 8890.
E-mail address: Matias.Rodriguez@anu.edu.au (M.D. Rodríguez).

0022-3093/$ – see front matter © 2011 Elsevier B.V. All rights reserved.
doi:10.1016/j.jnoncrysol.2011.10.028

Chemical etching has provided evidence of individual track formation above 35 keV/nm in $Fe_{81}B_{13.5}Si_{3.5}C_2$ [30], well above the threshold for damage creation obtained from electrical resistivity measurements. Systematic track etching experiments suggest that at this value of S_e the track damage is continuous and confined in a cylinder with a radius equal or larger than 3 nm [37]. It is important to note that chemical etching renders individual tracks visible for optical microscopes, but it involves the destruction of the track material. Scanning probe microscopy techniques provide visualization of individual tracks only on the surface [29,38,39], not in the bulk. Imaging tracks in amorphous materials by transmission electron microscopy (TEM) is extremely difficult when the irradiation is performed with monoatomic ions due to the lack of contrast [40] and has only yielded conclusive results when irradiating with cluster beams [41]. Due to their metastable configuration, artifact free imaging of amorphous metals is extremely difficult and has been reported in a study of their crystallization behavior [32].

In contrast to the various microscopic approaches described above, small angle scattering provides a powerful tool for quantitatively measuring the size and morphology of ion tracks in the bulk [42–44]. Tracks in amorphous metallic alloys were only studied for the case of $Pd_{80}Si_{20}$ using small angle neutron scattering (SANS) but no evidence for track formation was found [45]. Recently, SAXS has been successfully applied to resolve tracks in amorphous SiO_2 [43,46]. Here, we utilize SAXS to study the track morphology in amorphous metallic alloys ($Fe_{80}B_{20}$, $Fe_{85}B_{15}$, $Fe_{81}B_{13.5}Si_{3.5}C_2$ and $Fe_{40}Ni_{40}B_{20}$). Evidence for track formation has previously only been reported for $Fe_{85}B_{15}$ and $Fe_{81}B_{13.5}Si_{3.5}C_2$. Previously lacking evidence of ion track formation in $Fe_{80}B_{20}$ and $Fe_{40}Ni_{40}B_{20}$ and track radii are retrieved for all materials. We determine the track morphology and the formation threshold in these materials, confirming previous estimates deduced from the analysis of the evolution of electrical resistivity versus fluence in $Fe_{85}B_{15}$ [26,28].

2. Experimental

The metallic glasses were obtained in the form of ribbons, prepared by the melt spinning technique, with thicknesses between 15 and 29 μm. The nominal compositions, electronic and mass densities and thicknesses of the metals used for our experiments are listed in Table 1.

The ion tracks were produced by irradiating the materials at room temperature with 11.1 MeV per nucleon (MeV/u) ^{132}Xe, ^{152}Sm, ^{197}Au and 8.2 MeV/u ^{238}U ions at fluences between 1×10^{10} and 1×10^{12} ions/cm^2 at the UNILAC accelerator at GSI in Darmstadt, Germany. The corresponding energy losses exceed 36 keV/nm, leading to continuous track formation as expected from measurements of the chemical etching efficiency [30,37]. The ion beam was positioned normal to the surface of the samples. For such irradiation geometry and lower fluences (up to 3×10^{11} ions/cm^2), the amount track overlap can be considered as negligible. The extent of the track overlap in this work will be further discussed in the next section.

Table 1
Nominal compositions, electronic and mass densities and thicknesses of the amorphous metals used in this work.

Sample	Electronic density [10^{10} cm^{-2}]	Mass density [g/cm^3]	Thickness [μm]
$Fe_{80}B_{20}$ [a]	58.45	7.40	29 ± 1
$Fe_{85}B_{15}$ [b]	59.24	7.50	15 ± 1
$Fe_{81}B_{13.5}Si_{3.5}C_2$ [c]	57.92	7.32	29 ± 1
$Fe_{40}Ni_{40}B_{20}$ [d]	61.87	7.74	26 ± 1

[a] Supplied by Leibniz Institute for Solid State and Materials Research (IFW) Dresden.
[b] Supplied by Laboratoire de Physique de la Matière Condensée, Toulouse.
[c] Supplied by Goodfellow.
[d] Supplied by Vacuumschmelze Hanau Germany.

The ion track structure was studied using synchrotron SAXS performed in transmission geometry at the Australian Synchrotron. The X-ray energy was 12 keV, corresponding to a wavelength λ of 1.0332 Å. The distance between the sample and the Pilatus 1 M detector varied between ~980 and ~1690 mm and the absolute scattering was calibrated using a glassy carbon standard [47]. The samples were mounted on a three-axis goniometer for precision alignment. Measurements were taken with the ion tracks tilted between 0° and 10° with respect to the X-ray beam. Scattering images of $Fe_{81}B_{13.5}Si_{3.5}C_2$ irradiated with Au ions at 3×10^{11} ions/cm^2 are shown in Fig. 1. The high anisotropy of the image in Fig. 1(b) with tilted tracks confirms the high aspect ratio of the ion tracks that are only a few nanometres wide and extend through the entire sample thickness. Additionally, unirradiated samples were measured for background removal.

For analysis of the SAXS data, the scattering intensities corresponding to the tracks were extracted from the isotropic images of the aligned tracks (Fig. 1(a)), and by masking the streaks corresponding to the scattering of the tracks when tilted with respect to the X-ray beam (Fig. 1(b)). Both methods yield identical results. Simultaneously, the background was removed using the scattering spectrum of the unirradiated sample (example shown in Fig. 2(a)). Additionally, scattering intensities from images with tilted tracks were extracted in radial sectors excluding the streaks produced by the tracks. These were found to be identical to the images of the unirradiated samples, and we thus rule out additional contributions from spherical defects or fragmentation of the tracks on nanometer length-scales. The scattering originating from the ion tracks was modeled by parallel, well separated cylinders with length L and radius R. The scattering intensity

$$I(q) = C\cdot|\mathrm{F(q)}|^2 \tag{1}$$

can be expressed as a function of the scattering vector $q = \frac{4\pi}{\lambda}\sin(\theta)$, where λ is the X-ray wavelength, θ the scattering angle and F(**q**) is the scattering amplitude given in cylindrical coordinates by [48]

$$F(\mathbf{q}) = 4\pi\frac{\sin(q_z L/2)}{q_z}\int_0^\infty \rho(r)\,J_0(q_r r)r\,dr \tag{2}$$

where $\rho(r)$ is the radial electron density of the scattering object and J_0 is the zero order Bessel function, and q_r and q_z are the radial component and z-component of the scattering vector ***q***, respectively. The coefficient C in Eq. (1) contains information about the number density of the ion tracks *n*, the track volume *V* and the electron density change $\Delta\rho$ between track and matrix material:

$$C = n\,V^2\Delta\rho^2. \tag{3}$$

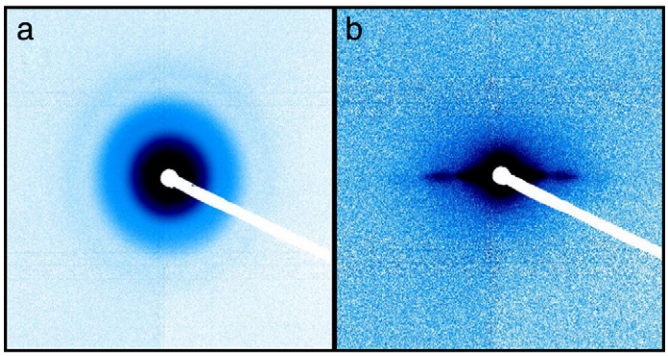

Fig. 1. SAXS images for $Fe_{81}B_{13.5}Si_{3.5}C_2$ irradiated with 11.1 MeV/u Au ions at 3×10^{11} ions/cm^2 with tracks aligned at 0° (a) and 10° (b) with respect to the X-ray beam.